DOI: 10.17344/acsi.2019.4988 *Acta Chim. Slov.* **2019,** *66,* 466–472

Scientific paper

Phase Equilibria in the $MnGa_2Te_4$-$MnIn_2Te_4$ System, Crystal Structure and Physical Properties of $MnGaInTe_4$

Faig Mamedagha Mammadov,[1] Imamaddin Rajabali Amiraslanov,[2] Yegana Rasul Aliyeva,[2] Sadiyar Sultan Ragimov,[2] Leyla Farkhad Mashadiyeva[1] and Mahammad Baba Babanly[1,*]

[1] *Institute of Catalysis and Inorganic Chemistry, Azerbaijan National Academy of Science, 113, H.Javid. ave., AZ-1143, Baku, Azerbaijan,*

[2] *Institute of Physics, Azerbaijan National Academy of Science, 131, H.Javid. ave., AZ-1143, Baku, Azerbaijan*

* *Corresponding author: E-mail: babanlymb@gmail.com*

Received: 03-01-2019

Abstract

The phase equilibria in the $MnGa_2Te_4$-$MnIn_2Te_4$ system were experimentally investigated by means of differential thermal analysis and powder X-ray diffraction technique. It was found that this system is quasi-binary and characterized by dystectic and eutectic equilibria and the formation of a wide area of solid solutions based on the starting compounds. The crystal structures of the $MnGaInTe_4$ and $MnIn_2Te_4$ were refined by the Rietveld method using powder X-ray diffraction data. It was established, that both phases crystallize in the tetragonal system (Space group *I-42m*). Electron paramagnetic resonance and Raman spectra, as well as the temperature dependences of the electrical conductivity and the Hall effect for the $MnGaInTe_4$ crystal, were studied.

Keywords: $MnGa_2Te_4$-$MnIn_2Te_4$ system; phase diagram; solid solutions; $MnGaInTe_4$ crystal structure; rietveld method; EPR spectroscopy; raman spectroscopy

1. Introduction

Complex metal chalcogenides are essential functional materials possessing optical, photoelectric, thermoelectric, magnetic and other properties.[1–7] Recent studies have shown that some of these phases are topological insulators and are considered promising for use in spintronics and quantum computing.[8–11] Among the chalcogenide materials, magnetic semiconductors of the type MB_2X_4 (where M – Mn, Fe, Co, Ni; B – Ga, In; X – S, Se, Te) and phases on their basis are very promising for use in the manufacture of lasers, light modulators, photodetectors and other electronic devices controlled by a magnetic field.[12–17]

Search and development of methods for the directed synthesis of new multicomponent phases and materials requires the study of phase equilibria in the relevant systems.[18,19] For this case, the systems including compounds which are structural or formula analogs are the greatest interest since the formation of broad areas of substitutional solid solutions can be expected in them.[20–24]

Herein, the phase equilibria in the $MnGa_2Te_4$-$MnIn_2Te_4$ system are studied, the crystal structures of the $MnGaInTe_4$ and $MnIn_2Te_4$ are refined, as well as the EPR and Raman spectra for the $MnGaInTe_4$ crystals are measured, and the temperature dependences of the electrical conductivity and the Hall Effect of the $MnGaInTe_4$ are investigated.

The starting compounds $MnGa_2Te_4$ and $MnIn_2Te_4$ were studied in detail. According to authors,[25] the $MnGa_2Te_4$ compound melts congruently at 1118 K (at 1093±10 K,[26]) and has a homogeneity region of 49.8–50.2 mol% MnTe over the MnTe-Ga_2Te_3 section. The $MnIn_2Te_4$ compound also melts congruently at 1013 K,[27] (at 1040 K according to reference,[28]).

The crystal structure of the $MnGa_2Te_4$ was studied in a number papers.[26, 29, 30] The authors,[29] showed that this compound has a pseudo-tetragonal monoclinic unit cell with parameters: $a = b = 0.847$ nm; $c = 4.83$ nm; $\alpha = \beta = \gamma \sim 90°$; $Z = 16$. Close parameters were obtained: $a = b = 0.8486$

nm; c = 4.840 nm; α = β = γ ~ 90°; Z = 16.[26] The crystal structure of $MnGa_2Te_4$ was studied by the Laue method.[30] It was shown that this compound crystallizes in the monoclinic structure (Sp. gr. *C2/c*) with parameters: a = 1.1999(3); b = 1.1999(3); c = 2.4922(6) nm; β = 104.01(2)°; Z = 16.

The $MnIn_2Te_4$ compound crystallizes in a tetragonal structure (Sp. Group $I\ \bar{4}2m$) with the parameters: a = 0.6191(2) nm; c = 1.2382(3) nm; Z = 2.[31]

Mn-00003

2. The Experimental Part

2. 1. Synthesis

For research ternary compounds $MnGa_2Te_4$ and $MnIn_2Te_4$ were synthesized. Simple substances from the company EVOCHEM ADVANCED MATERIALS GMBH (Germany) of high purity were used for the synthesis: gallium ingots (Ga-00009; 99.999%), indium in granules (In-00005; 99.999%), manganese pieces (Mn-00003; 99.98%), tellurium pieces (Te-00005; 99.9999%). The synthesis was carried out by melting of elemental components in stoichiometric ratios in evacuated to about 10^{-2} Pa quartz ampoules at temperatures ~50 K higher than their melting points followed by slow cooling in the furnace off mode to room temperature. In order to prevent the interaction of quartz with manganese, the synthesis of compounds and alloys of the studied system was carried out in graphitized ampoules.

The individuality of the synthesized compounds was controlled by differential-thermal analysis (DTA) and powder X-ray diffraction technique (PXRD). According to the DTA data, the $MnGa_2Te_4$ and $MnIn_2Te_4$ compounds melt congruently correspondingly at 1075 ± 3 K and 1021 ± 3 K, which is somewhat different from the literature data.[25–28] Analysis of the powder X-ray diffraction patterns confirmed the single-phase of both compounds.

The $MnGa_2Te_4$-$MnIn_2Te_4$ alloys were prepared from the starting ternary compounds also by vacuum alloying in graphitized quartz ampoules. All alloys were subjected to thermal annealing at 900 K for 500 hours in order to achieve complete homogenization and then slowly cooled in the furnace off.

2. 2. Methods

Phase equilibria in the $MnGa_2Te_4$-$MnIn_2Te_4$ system were investigated by means of DTA and PXRD methods.

DTA of the equilibrated alloys was carried out using a NETZSCH 404 F1 Pegasus system. The measurement was performed between room temperature and ~1300 K with a heating and cooling rate of 5 K · min^{-1} under the inert gas (Ar) flow. Temperatures of thermal effects were determined from the heating curves with an accuracy of ± 2 K. NETZSCH Proteus Software was used for measuring and evaluating data.

Scanning Electron Microscopy combined with Energy-Dispersive X-ray spectroscopy (SEM/EDXS) was used for elemental analysis of samples. SEM/EDXS was performed using a JEOL JSM 6610-LV Scanning Electron Microscope.

The PXRD analysis was performed using a "D2 Phaser" diffractometer with $CuK\alpha_1$ radiation (5°≤2-theta≤120°). The solution and refinement of the crystal structure were done by the Rietveld method using the TOPAS-4.2 Software (Bruker).

Electron Paramagnetic Resonance (EPR) spectroscopy of $MnGaInTe_4$ crystals was carried out with the ELEXSYS E 580 spectrometer (Bruker), and the Raman spectra were obtained using the "Nanofinder 30" 3D Laser Raman Microspectroscopy System (Tokyo Instruments).

The temperature dependences of the electrical conductivity and the Hall effect for the $MnGaInTe_4$ were studied in the temperature range 100–400 K on the "HL5500 PC-Hall effect measurement system" (Nanometric).

3. Results and Discussion

3. 1. Phase equilibria in the $MnGa_2Te_4$-$MnIn_2Te_4$ system

From the DTA data (Table 1) and PXRD studying of annealed $MnGa_2Te_4$-$MnIn_2Te_4$ alloys, it is established that this system is characterized by the dystectic (D) and eutectic (e) equilibria (Fig. 1a). The β-phase of the $MnGaInTe_4$ composition melts with an open maximum at 1028 K. The eutectic has a composition of 30 mol% $MnIn_2Te_4$ and crystallizes at 1012 K. Wide regions of solid substitutional solutions based on starting compounds are formed. At the

Table 1. Experimental DTA and PXRD data for the $MnGa_2Te_4$-$MnIn_2Te_4$ system

Composition, mol% $MnIn_2Te_4$	The thermal effect, K	Parameters of the tetragonal lattice, nm	
		a	c
0 ($MnGa_2Te_4$)	1083		
10	1030–1062		
15	1013–1050		
20	1012–1034	0.60816(3)	1.21308(8)
25	1012		
30	1011–1016	0.60812(3)	1.21310(8)
35	1013–1020		
40	1018–1024	0.60852(3)	1.21403(8)
45	1026		
50	1030	0.610293 (7)	1.21766(2)
60	1013–1023	0.61207(3)	1.22232(7)
70	1004–1011		
80	1000	0.61553(3)	1.23026(7)
90	1005–1012		
100 ($MnIn_2Te_4$)	1022	0.61949(5)	1.23956(2)

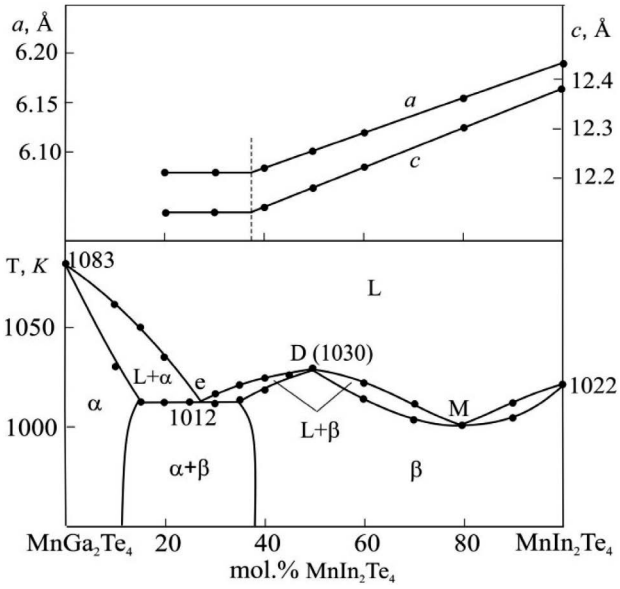

Fig. 1. The phase diagram of the $MnGa_2Te4$-$MnIn_2Te_4$ system and the concentration dependences of the crystal lattice parameters of the β-phase

eutectic temperature the solubility based on $MnGa_2Te_4$ (α-phase) is 15 mol%, and on the basis of $MnIn_2Te_4$ is 65 mol% (β-phase). On the liquidus and solidus curves of the β-phase there is a minimum point (M) at 1000 K. The congruent melting of both starting compounds, the presence of the invariant three-phase eutectic equilibrium L ↔ α + β and the extreme points D and M, as well as the absence of multiphase areas on the phase diagram, show the quasi-binary nature of this system.

PXRD results confirmed the formation of broad areas of solid solutions in the system. Figure 2 shows that powder diffraction images of the alloys from 40–100 mol% $MnIn_2Te_4$ composition area are qualitatively identical with the diffraction pattern for pure $MnIn_2Te_4$ and characterized by a certain shift of reflection lines with composition changing. The PXRD pattern of the alloy with composition 20 mol% $MnIn_2Te_4$ consists of reflection lines of both phases $MnGa_2Te_4$ (α-phase) and $MnIn_2Te_4$ (β-phase).

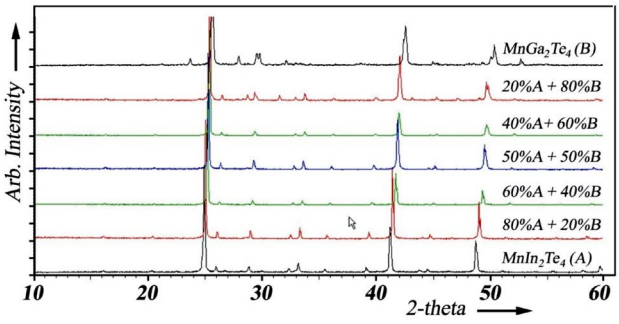

Fig. 2. PXRD patterns for some alloys of the $MnGa_2Te_4$-$MnIn_2Te_4$ system

The concentration dependence of the parameters of the crystal lattice (Table 1, Fig. 1b) of the β-phase has linear character and allows refining the region of its homogeneity at room temperature (38 mol% $MnIn_2Te_4$).

3. 2. Crystal structure of $MnIn_2Te_4$ and $MnGaInTe_4$

Based on the PXRD data, we determined the crystallographic characteristics of the $MnIn_2Te_4$ and $MnGaInTe_4$ samples (Table 2). PXRD patterns for $MnIn_2Te_4$ and $MnGaInTe_4$ and the intensities differences between the experimental and calculated by Rietveld method data are shown in Fig.3. The obtained results show good agreement of symmetry and cell parameters of these samples with the corresponding characteristics.[31] The indexing of the diffraction patterns based on obtained crystallographic parameters showed that the studied samples are single-phase. Comparison of the unit cell parameters of $MnIn_2Te_4$ and $MnGaInTe_4$ shows a noticeable difference in their values ($\Delta a \sim 0.0092$ nm; $\Delta c \sim 0.0219$ nm), which exceeds the value of errors many times. This clearly confirms the entry of Ga atoms into the structure. Despite solving the crystal structure of $MnIn_2Te_4$ on the basis of single crystals data,[31] we also used their results to refine the structure of this compound, but on the basis of powder data and the Rietveld method. The above results were also used to refine the structure of the compound $MnGaInTe_4$ by the Rietveld method. The Mn and In atoms in the structure are located in identical positions statistically, where the ratio of the number of Mn atoms to In is 1:2.[31] This structure belongs to the defective type of chalcopyrite and all metals are located in the tetrahedron of tellurium atoms. In order to refine the crystal structures of $MnIn_2Te_4$ and $MnGaInTe_4$, first, for both compounds, the Lebail and Pawley methods were used to approximate the profiles of the diffraction peaks and to refine the unit cell parameters. For both methods, the obtained results turned out to be almost identical. Later, on the basis of the obtained diffraction data, the crystal structures of the noted compounds were refined. The final results are presented in Tables 2-4. Figure 4 shows a three-dimensional presentation of the crystal structure of these phases.

Table 2. Refined structure parameters for $MnIn_2Te_4$ and $MnGaInTe_4$

Structure parameters	$MnIn_2Te_4$	$MnGaInTe_4$
Space group	*I*-42m	*I*-42m
Cell parameters: *a* (nm)	0.619490(5)	0.610293 (7)
c (nm)	1.23956(2)	1.21766(2)
The cell volume (nm^3)	0.47583(3)	0.453528(13)
Density (g/cm^3)	5.56 (2)	5.50 (2)
R-LeBail (%)	0.406	0.155
R-Pawley (%)	0.435	0.171
R-Bragg (%)	1.898	0.235

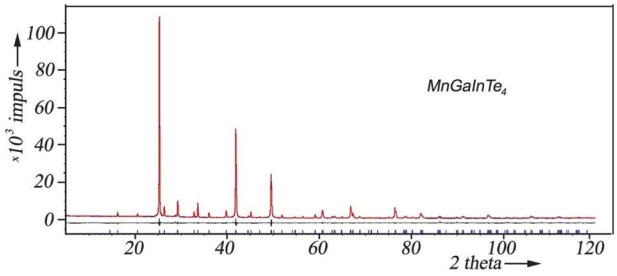

Fig. 3. PXRD patterns of $MnIn_2Te_4$ and $MnGaInTe_4$. The difference between the experimentally obtained and calculated by the Rietveld method intensities is given under the X-ray diffraction spectrum

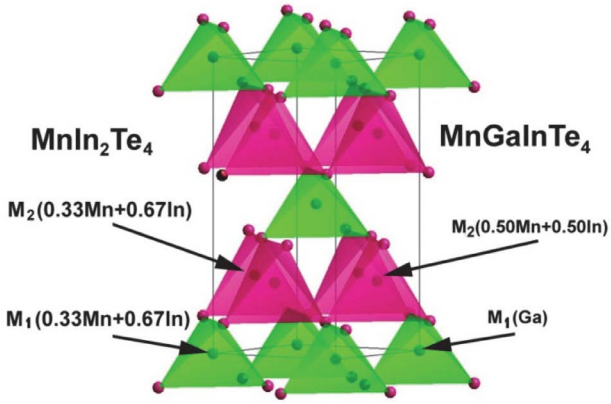

Fig. 4. Occupancy of metal positions in $MnIn_2Te_4$ and $MnGaInTe_4$ crystal structures

The results of the elemental analysis (Table 5) and X-ray fluorescence spectrum of $MnGaInTe_4$ crystals (Fig. 5) are in good agreement with the chemical formula.

Table 5. Elemental analysis results for $MnGaInTe_4$

Element	Weight %	Atomic %
Mn *K*	7.03	13.76
Ga *K*	9.26	14.27
In *L*	15.74	14.73
Te *L*	67.97	57.24
Total	**100.00**	**100.0**

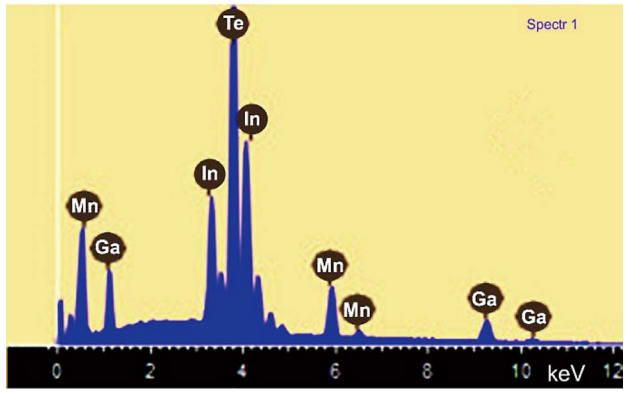

Fig. 5. The XRF spectrum for the $MnGaInTe_4$ crystal

Table 3. Atomic positional parameters in the $MnIn_2Te_4$ crystal

Atoms	Multiplicity and Wyckoff letter	x	y	z	Atom type and relative occupation	B_{eq}, (nm^2)
M_1(In+Mn)	2a	0	0	0	Mn^{+2} 0.33(1)	0.005 (1)
In^{+3} 0.67(1)						0.005 (1)
M_2(In+Mn)	4d	0	0.5	0.25	Mn^{+2} 0.33(1)	0.009 (1)
					In^{+3} 0.67(1)	0.009 (1)
Te	8i	0.2756(2)	0.2756(2)	0.1142(1)	Te 1	1.001(1)
Interatomic distances (nm)		$M_1(In_1, Mn_1)$ – Te = 0.2772(1)			$M_2(In_2,Mn_2)$ – Te = 0.2800(1)	

Table 4. Atomic positional parameters in the $MnGaInTe_4$ crystal

Atoms	Multiplicity and Wyckoff letter	x	y	z	Atom type and relative occupation	B_{eq}, (nm^2)
Ga	2a	0	0	0	Ga^{3+} 1.018(26)	0.006(3)
M(In+Mn)	4d	0	0.5	0.25	In^{3+} 0.495(22)	0.007(1)
					Mn^{2+} 0.505(22)	0.007(1)
Te	8i	0.2651(4)	0.2651(4)	0.1129(2)	Te 1	0.008(1)
Interatomic distances (nm)		Ga – Te =0.2669(3)			M(In, Mn) – Te = 0.2731(1)	

As can be seen from Tables 3 and 4, and also from Fig. 4, the crystal lattices of $MnIn_2Te_4$ and $MnGaInTe_4$ differ significantly in the occupancy of crystallographic positions. In the $MnIn_2Te_4$ structure, the *2a* and 4d positions are occupied in ratio 1:2 by the Mn and In atoms. In the structure, positions *2a* are completely occupied by gallium atoms, and the Mn and In atoms are statistically located in *4d* positions with a 1:1 ratio. The localization of Ga atoms in position *2a* in $MnGaInTe_4$ is apparently due to the fact that the ionic radius of Ga^{3+} is noticeably smaller (~ 0.018 nm) of the ionic radius of In^{3+}. Such occupancy of crystallographic positions in the $MnGaInTe_4$ phase allows us to characterize it as an ordered solid solution based on the $MnIn_2Te_4$ compound. This is in good agreement with the phase diagram (Fig. 1a), according to which the stoichiometric composition of $MnGaInTe_4$ corresponds to the dystectic point D.

3. 3. Physical Properties of the $MnGaInTe_4$

3. 3. 1. EPR Spectrum of $MnGaInTe_4$ Crystal

In fig. 6 showing the EPR spectrum of MnGaInTe4 crystals, where only one broad peak is observed. Based on the composition of this phase, it is clear that this peak refers to the resonant frequencies of manganese. If in the structure the smallest distances between Mn atoms are

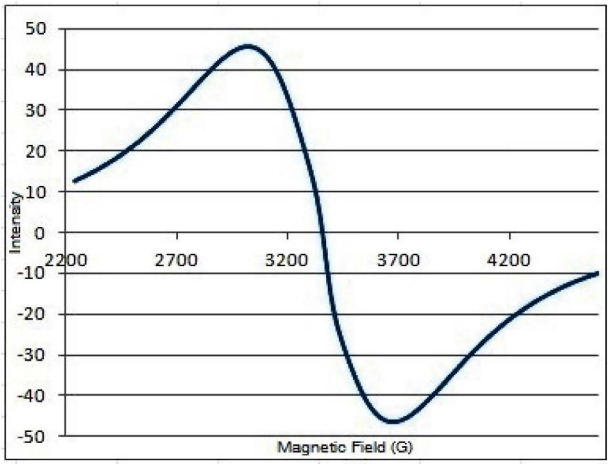

Fig. 6. EPR spectrum for the $MnGaInTe_4$ crystal

more than 1 *nm*, then their EPR spectra are characterized by a fine structure consisting of six nearby lines. However, the decrease in the distances between these paramagnetic ions leads to the merging of these fine lines to a single broad peak.[32] In our case, the distance between the Mn atoms is equal to the translational parameter of the cell ***a*** (***a*** = 0.610293 *nm*), which is significantly less than 1 *nm*. Consequently, the EPR spectrum should consist of one broad peak, which was confirmed experimentally.

3. 3. 2. Raman Spectrum of $MnGaInTe_4$ Crystal

The Raman spectrum for the $MnGaInTe_4$ crystal was represented in Fig.7. As can be seen three peaks at 96, 119 and 139 cm^{-1} are observed in the low-frequency region of the spectrum. Raman spectra of $CdIn_2Te_4$, $ZnIn_2Te_4$, and $MnIn_2Te_4$ were studied by authors of,.[33] All these compounds crystallize in the tetragonal system and their structures such as $MnGaInTe_4$ belong to the defective type of chalcopyrite.[34] This closeness is well reflected in their Raman spectra (Table 6). As is seen from Table 6 the overall characteristics of the spectra of $MnGaInTe_4$ are the same as its ternary analogs. Some distinction between the frequencies of the Raman-active modes of these materials is due to the difference in their chemical composition.

Table 6. Raman spectra data for $MnGaInTe_4$ and some of its structural analogs

Phase	Raman peaks, (cm^{-1})		
$MnGaInTe_4$	96	119	139
$MnIn_2Te_4$ [33]	97	123	153
$CdIn_2Te_4$ [33]	102	128	159
$ZnIn_2Te_4$ [33]	100	123	143; 155

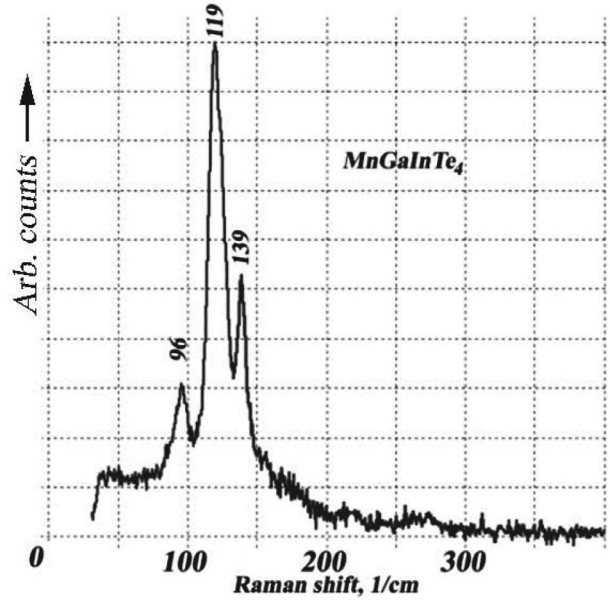

Fig. 7. Raman spectrum for the $MnGaInTe_4$ crystal

3. 3. 3. Conductivity and Hall Effect of the $MnGaInTe_4$ Crystal

The temperature dependences of the electrical conductivity (Fig. 8a) and the Hall effect (Fig. 8b) for the $MnGaInTe_4$ in the temperature range 100–400 K were studied. The value of electrical conductivity increases with increasing temperature. However, above 300 K, the electrical conductivity begins to increase more sharply. The sign of the

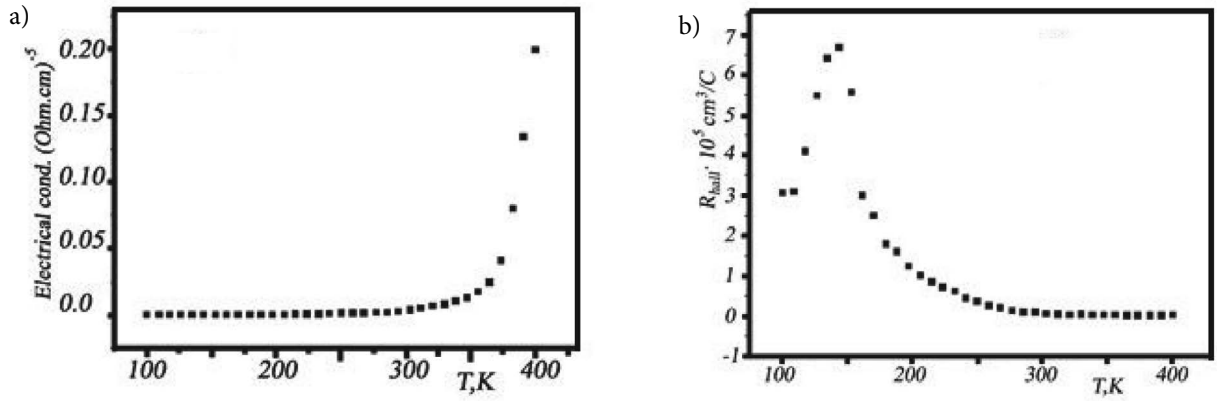

Fig. 8. The temperature dependences of the electrical conductivity (a) and the Hall Effect (b) for the $MnGaInTe_4$ crystal

Hall coefficient indicates the hole type of conductivity in the entire range of temperatures of 100-400 K. The hole concentration at room temperature calculated from measurements of the Hall coefficient is $p = 1.25 \cdot 10^{15}$ cm^{-3}. The dependence R_{Hall} (T) passes through a maximum at the 140 K and then decreases with increasing temperature (Fig. 8b).

In the literature, we did not find any information about the electrical conductivity and Hall Effect in $MnGa_2Te_4$ and $MnGaInTe_4$ compounds. Only,[35] reports the energy gap width of $MnGa_2Te_4$ E_g is 1.52 eV at 300K, which is determined from optical measurements. The determination of E_g for $MnGaInTe_4$ compounds from our measurements is impossible since its expected temperature region of intrinsic conductivity is much higher than 400 K. The presence of a maximum on the temperature dependence of the Hall coefficient for $MnGaInTe_4$ may be explained by the impurity band existence. At temperatures above T_{max}, charge transfer is performed by holes in the valence band. Below the maximum temperature, the transfer is carried primarily by thermally activated jumps between the acceptors.

The decrease in the value of the Hall coefficient above T_{max} with increasing temperature indicates an increase in the concentration of charge carriers. As a result, an increase in the value of electrical conductivity is observed (Fiq.8a). With increasing temperature, the activated electrons from the valence band are captured at these levels and become increasing of concentration of holes. The activation energy E_a has estimated from the temperature dependences of electrical conductivity was about 28 meV.

4. Conclusion

The $MnGa_2Te_4$-$MnIn_2Te_4$ quasi-binary system is characterized by a phase diagram with dystectic and eutectic equilibria and the formation of broad regions of solid solutions with a monoclinic structure (0-12 mol% $MnIn_2Te_4$) and a defect structure of chalcopyrite (38-100 mol% $MnIn_2Te_4$). Using powder X-ray diffraction data by means of the Rietveld method the crystal structures of the $MnGaInTe_4$ and $MnIn_2Te_4$ were refined. It was established, that both phases crystallize in the tetragonal system (Space group *I-42m*), but they differ significantly in the occupancy of the crystallographic positions. This allows characterizing $MnGaInTe_4$ as an individual chemical compound, which is in accordance with the phase diagram. Comparison of Raman peaks of $MnGaInTe_4$ with isostructural compounds MIn_2Te_4 (M = Zn, Mn, Cd) showed that the overall characteristics of the spectra are the same and differ only in values of the peaks frequencies. The observed EPR signal for $MnGaInTe_4$, consisting of one broad peak, indicates the presence of long-range ordering in the arrangement of Mn atoms, which is in accordance with the crystallographic data. The Hall effect study was used to determine the type of conductivity and the concentration of holes in $MnGaInTe_4$ crystals.

5. Acknowledgment

This work was supported by the Science Development Foundation under the President of the Republic of Azerbaijan – **Grant № EİF-BGM-4-RFTF-1/2017-21/11/4-M-12**

6. References

1. G. K. Ahluwalia (Ed.), Applications of Chalcogenides: S, Se, and Te, Springer, **2016**.
2. A. V. Kolobov, J. Tominaga, Two-Dimensional Transition-Metal Dichalcogenides, Springer International Publishing, **2016**.
3. I. Chung, M. G. Kanatzidis, Chem. Mater. **2014**, *26*, 849–869. **DOI:**10.1021/cm401737s
4. M.-R. Gao, Y.-F. Xu, J. Jiang, S.-H. Yu, Chem. Soc. Rev. **2013,** *42,* 2986–3017. **DOI:**10.1039/C2CS35310E.

5. B. Sa, Z. Sun Z, B. Wu, *Nanoscale*. **2016**, *8,* 1169–1178. **DOI:**10.1039/C5NR06871A
6. X. Congxin, L. Jingbo, *J. Semicond*. **2016,** *37*, 051001-1–051001-9. **DOI:**10.1088/1674-4926/37/5/051001
7. C. Gayner, K. K. Kar, *Prog. Mater. Sci.* **2016**, *83*, 330–382. **DOI:**10.1016/j.pmatsci.2016.07.002
8. S. V. Eremeev, G. Landolt, T. V. Menshchikova, V. Slomski, Y. M. Koroteev, Z. S. Aliev, M. B. Babanly, J. Henk, A. Ernst, L. Patthey, A. Khajetoorians, J. Wiebe, P. M. Echenique, S. S. Tsirkin, I. R. Amiraslanov, J. H. Dil, E. V. Chulkov, *Nat. Commun*. **2012**, *3*, 635–638. **DOI:**10.1038/ncomms1638
9. M. Papagno, S. Eremeev, J. Fujii, Z. S. Aliev, M. B. Babanly, S. Mahatha, I. Vobornik, N. Mamedov, D. Pacile, E. V. Chulkov, *ACS Nano.* **2016,** *10*, 3518–3524. **DOI:**10.1021/acsnano.5b07750
10. L. Viti, D. Coquillat, A. Politano, K. A. Kokh, Z. S. Aliev, M. B. Babanly, O. E. Tereshchenko, W. Knap, E. V. Chulkov, M. S. Vitiello, *Nano Lett*. **2016,** *16*, 80–87. **DOI:**10.1021/acs.nanolett.5b02901
11. I. A. Shvets, I. I. Klimovskikh, Z. S. Aliev, M. B. Babanly, J. Sánchez-Barriga, M. Krivenkov, A. M. Shikin, E. V. Chulkov, *Phys. Rev*. B. **2017,** *96*, 235124–7. **DOI:**10.1103/PhysRevB.96.235124
12. B. R. Myoung, J. T. Lim, C. S. Kim, *J. Magn. Magn. Mater*. **2017,** *438*, 121–125. **DOI:**10.1016/j.jmmm.2017.04.056.
13. Memo, W. Kwarteng-Acheampong, H. Heauseler, *Mater.Res. Bull*. **2003,** *38*, 1057–1061. **DOI:**10.1016/S0025-5408(03)00079-5
14. T. Torres, V. Sagredo, L. M. de Chalbaund, G. Attolini, F. Bolzoni, *Phys. B: Condensed Matter*, **2006,** *384,* 100–102. **DOI:**10.1016/j.physb.2006.05.162
15. N. A. Moroz, J. S. Lopez, H. Djieutedjeu, K. G. Ranmohotti, A. Olvera, P. Ren, *Chemistry of Materials*, **2016,** *28*, 8570–8579. **DOI:**10.1021/acs.chemmater.6b03293
16. R. Cadenasa, M. Quintero, E. Quintero, R. Tovar, M. Morocoima, J. Gonzalez, J. Ruiz, J. M. Broto, H. Rakoto, J. C. Woolley, G. Lamarche, *Physica B.* **2004,** *346–347*, 413–415. **DOI:**10.1016/j.physb.2004.01.117
17. F. López-Vergara, A. Galdámez , V. Manríquez, P. Barahona, and O. Peña, *Phys. Status Sol.B.* **2014,** *251*, 958–964. **DOI:**10.1002/pssb.201350038
18. P. Villars, A. Prince, H. Okamoto, Handbook of Ternary Alloy Phase Diagrams (10 volume set), American Technical Publishers, **1995**
19. M. B. Babanly, E. V. Chulkov, Z. S. Aliev, A. V. Shevel'kov, I. R. Amiraslanov, *Russ. J. Inorg. Chem*. **2017,** *62*, 1703–1729. **DOI:**10.1134/S0036023617130034
20. S. Z. Imamaliyeva, D. M. Babanly, D. B.Tagiev, M. B. Babanly, *Russ. J. Inorg.Chem.,* **2018**, *13*, 1703–1027. **DOI:**10.1134/S0036023618130041
21. I. J. Alverdiyev, Z. S. Aliev, S. M. Bagheri, L. F. Mashadiyeva, Y. A. Yusibov, M. B. Babanly, *J. Alloys Compd*. **2017,** *691*, 255–262. **DOI:**10.1016/j.jallcom.2016.08.251
22. Imamaliyeva S. Z., Gasanly T. M., Gasymov V. A., M. B. Babanlı, *Acta Chim. Slov.* **2017**, *64*, 221–226. **DOI:** 10.17344/acsi.2017.3207
23. Imamaliyeva S. Z., Alakbarzade G. I., Mahmudova M. A., Amiraslanov I. R., M. B. Babanly, *Acta Chim.Slov.* **2018**, *65,* 365–371. **DOI:**10.17344/acsi.2017.4053
24. F. M. Mammadov, S. Z. Imamaliyeva, I. R. Amiraslanov, M. B. Babanly, *Condensed matter and interphases*, **2018**, *20,* 604–610. **DOI:**10.17308/kcmf.2018.20/633
25. P. G. Rustamov, B. K. Babayeva, D. S. Ajdarova, *Azerb.Chem. Journ*. **1978,** *5*, 112–114 (in Russian).
26. L. Garbato, A. Geddo-Lehmann, F. Ledda, M. Cannas, O. Devoto, *Jpn. J. Appl. Phys*. **1993,** *32*, 389–390. **DOI:**10.7567/JJAPS.32S3.389
27. J. T. Kelliher, K. J. Bachmann, *MRS Proceedings.* **1990,** *216,* 479–482. doi:10.1557/proc-216-479
28. B. K. Babayeva, P. G. Rustamov, *Azerb.Chem.Journ*. **1983,** *2,* 124–127 (in Russian).
29. K.-J. Range, H.-J. Hubner, Z. *Naturforsch*. **1976,** *31b*, 886–887. **DOI:**10.1515/znb-1976-0632
30. M. Cannas, A. Garbato, L. Garbato, F. Ledda, G. Navarra, *Prog. Cryst. Growth Charact. Mater*. **1996,** *32*, 171–183. **DOI:**10.1016/0960-8974(95)00020-8 .
31. K.-J.Range, H.-J.Hubner, Z. *Naturforsch.* B. **1975,** *30*, 145–148. **DOI:**10.1515/znb-1975-3-401 .
32. S. Jain, M. Willander, R. Van Overstraeten, Compound Semiconductors Strained Layers and Devices, Springer Science, Business Media, LLC, **2000**.
33. J.-F. Lambert, P.V. Huong, J. Limtraku, J.-C. Launay, *J. Mol. Struct*. **1993,** *294*, 159–162. **DOI:**10.1016/0022-2860(93)80339-W
34. H. Hahn, G. Frank, A. D. Stoerger, W. Klingler, G. Stoerger, *Z. Anorg. Allg. Chem*. **1955,** *279*, 241–270. **DOI:**10.1002/zaac.19552790502
35. G. A. Medvedkin, Yu.V. Rud, M. A. Tairov, *Phys. stat. sol.* (a). **1988,** *110***,** 631–643. **DOI:**10.1002/pssa.2211100236

Povzetek

Fazno ravnotežje v sistemu $MnGa_2Te_4$-$MnIn_2Te_4$ smo eksperimentalno raziskali s pomočjo diferencialne termične analize in rentgenske praškovne difrakcije. Ugotovili smo, da je ta sistem kvazi-binaren in ima karakteristična distetična in evtektična ravnotežja ter široka območja trdnih raztopin na osnovi izhodnih spojin. Kristalni strukturi $MnGaInTe_4$ in $MnIn_2Te_4$ smo določili z Rietveldovo metodo z uporabo podatkov rentgenske praškovne difrakcije. Ugotovili smo, da obe fazi kristalizirata v tetragonalnem kristalnem sistemu (prostorska skupina *I-42m*). Kristale $MnGaInTe_4$ smo preučevali tudi z elektronsko paramagnetno resonanco (EPR), ramansko spektroskopijo in meritvami električne prevodnosti v odvisnosti od temperature.